Published in final edited form as:
Heart Rhythm. 2010 June ; 7(6): 771–778. doi:10.1016/j.hrthm.2010.01.032.

Sudden Infant Death Syndrome-Associated Mutations in the Sodium Channel Beta Subunits

Bi-Hua Tan, MD, PhD[*], **Kavitha N Pundi, MD**[*], **David W Van Norstrand, BS**[*], **Carmen R Valdivia, MD**, **David J Tester, BS**, **Argelia Medeiros-Domingo, MD, PhD**, **Jonathan C. Makielski, MD**, and **Michael J. Ackerman, MD, PhD**
Departments of Medicine, Pediatrics, and Molecular Pharmacology & Experimental Therapeutics/ Divisions of Cardiovascular Diseases and Pediatric Cardiology, Mayo Clinic, Rochester, MN (KNP, DWV, DJT, AMD, and MJA), Division of Cardiovascular Medicine, Department of Medicine, University of Wisconsin, Madison, WI (BHT, CRV, JCM)

Abstract

Background—Approximately 10% of sudden infant death syndrome (SIDS) may stem from potentially lethal cardiac channelopathies, with approximately half of channelopathic SIDS involving the $Na_V1.5$ cardiac sodium channel. Recently, Na_V beta subunits have been implicated in various cardiac arrhythmias. Thus, the four genes encoding Na_V beta subunits represent plausible candidate genes for SIDS.

Objective—To determine the spectrum, prevalence and functional consequences of sodium channel beta subunit mutations in a SIDS cohort.

Methods—In this IRB-approved study, mutational analysis of the 4 beta subunit genes: *SCN1B – 4B* was performed using PCR, DHPLC, and direct DNA sequencing of DNA derived from 292 SIDS cases. Engineered mutations were co-expressed with SCN5A in HEK 293 cells, and whole cell patch clamped. One of the putative SIDS-associated mutations was similarly studied in adenovirally transduced adult rat ventricular myocytes.

Results—3 rare (absent in 200–800 reference alleles) missense mutations (β3-V36M, β3-V54G and β4-S206L) were identified in 3/292 SIDS cases. Compared to SCN5A+β3-WT, β3-V36M significantly decreased peak I_{Na} and increased late I_{Na} while β3-V54G resulted in a marked loss-of-function. β4-S206L accentuated late I_{Na} and positively shifted the midpoint of inactivation compared to SCN5A+β4-WT. In native cardiomyocytes, β4-S206L accentuated late I_{Na} and increased the ventricular action potential duration (APD) compared to β4-WT.

Conclusion—This study provides the first molecular and functional evidence to implicate the Na_V beta subunits in SIDS pathogenesis. Altered $Na_V1.5$ sodium channel function due to beta subunit mutations may account for the molecular pathogenic mechanism underlying approximately 1% of SIDS.

Keywords

Genetics; Beta subunits; Ion channel; SCN5A; SIDS

Address for correspondence: Michael J. Ackerman, M.D., Ph.D., Mayo Clinic Windland Smith Rice Sudden Death Genomics Laboratory, Guggenheim 501, Mayo Clinic, Rochester, MN 55905, 507-284-0101 (phone), 507-284-3757 (fax), ackerman.michael@mayo.edu.
[*]BHT, KNP, and DWV contributed equally to this manuscript and are co-equal first authors

INTRODUCTION

Sudden infant death syndrome (SIDS) is defined as the sudden death of an infant under the age of one that remains unexplained after a thorough case investigation including medical autopsy, death scene investigation and detailed review of the clinical history.[1] Despite the successes of the National "Back to Sleep" Campaigns, over 2000 infants each year die from SIDS.[2] SIDS is rare during the first month of life and although it can occur in older infants, most SIDS deaths occur by the end of the sixth month, with the greatest number between 2 and 4 months of age.

While the pathogenic mechanisms of SIDS still remain largely unexplained, it is estimated that approximately 10% of SIDS stems from cardiac channelopathies, including congenital long QT syndrome (LQTS), short QT syndrome (SQTS), Brugada syndrome (BrS), and catecholaminergic polymorphic ventricular tachycardia (CPVT), which can result in dysrhythmia and sudden cardiac death.[3–8] Approximately half of these channelopathic deaths involve the $Na_V1.5$ cardiac sodium channel (SCN5A) encoded by *SCN5A*,[3, 6, 8, 9] where gain-of-function mutations result in LQT3[10–12] and loss-of-function mutations result in BrS1.[13]

$Na_V1.5$ is a highly regulated macromolecular complex, with associated partner proteins also implicated in disease pathogenesis including caveolin-3 in LQTS and SIDS,[14, 15] GPD1L in BrS and SIDS,[16, 17] α1-syntrophin in LQTS and SIDS,[18, 19] and ankyrin G in BrS.[20] $Na_V1.5$ is also highly regulated by its beta subunits, which also have been recently implicated in arrhythmias including BrS,[21, 22] cardiac conduction disease (CCD),[22] atrial fibrillation (AF),[23] idiopathic ventricular fibrillation (IVF),[24] and LQTS.[25]

Based on these recent findings and considering that perturbations involving $Na_V1.5$ are more common in channelopathic SIDS compared to LQTS, we hypothesized that mutations in the Na_V beta subunits may result in some cases of SIDS through dysregulation of $Na_V1.5$. Therefore, the objective of our study was to determine the spectrum and prevalence of mutations in the genes encoding the cardiac sodium channel beta subunits (β1–4) in a large cohort of SIDS.

METHODS

SIDS cohort

292 SIDS cases derived from population-based cohorts of unexplained infant deaths (114 female infants, 177 male infants, 1 unknown; 203 white, 76 African American, 10 Hispanic, 2 Asian, 1 unknown; average age, 2.9 ± 1.9 months; range, 6 hours - 12 months) were submitted to the Mayo Clinic Windland Smith Rice Sudden Death Genomics Laboratory for postmortem genetic testing. Enrollment criterion was autopsy-negative sudden unexplained death of an infant < 1 year of age. By definition, the death had to be unexplained even after a comprehensive medico-legal autopsy. The study was approved by the Mayo Foundation Institutional Review Board as an anonymous necropsy study. Therefore, only limited medical information such as the sex, ethnicity and age of the infant at the time of death was generally available.

Beta subunit mutational analysis

DNA was extracted from autopsy blood with the Puregene DNA Isolation Kit (Gentra, Minneapolis, Minn) or from frozen necropsy tissue with the Qiagen DNeasy Tissue Kit (Qiagen, Inc, Valencia, Calif). Mutational analysis of all 19 translated exons of the beta subunit genes *SCN1B*, *SCN2B*, *SCN3B*, and *SCN4B* was performed using polymerase chain reaction (PCR) and denaturing high performance liquid chromatography (DHPLC) after design of intronic primers to amplify all translated exons. Abnormal DHPLC profiles were then sequenced to determine the nature of the amino-acid substitution. Reference alleles, derived

from healthy adult control subjects whose ethnicity matched the decedent, were also examined by DHPLC to determine whether an identified amino acid variant was a common polymorphism. Primer sequences, PCR conditions and DHPLC conditions are available upon request.

To be considered a possible SIDS-associated mutation, the genetic variant had to (1) be a non-synonymous variant (synonymous single-nucleotide polymorphisms were excluded from consideration), (2) involve a highly conserved residue, (3) be absent in reference alleles from healthy ethnic-matched control subjects, and (4) yield a functionally altered, pro-arrhythmic cellular phenotype consistent with a potentially lethal arrhythmogenic substrate.[16]

Site-directed mutagenesis and heterologous expression

The mutations in beta subunits were created by site-directed mutagenesis (mutagenesis kit from Stratagene, La Jolla, California, USA) using a PCR technique in the pcDNA3 vector (Invitrogen, Carlsbad, California, USA). Mutations were then subcloned into pIRES2-EGFP vector (Clontech Laboratories, Palo Alto, California, USA) and an entry vector of pENTR1A-IRES2EGFP.[19] Integrity of the constructs was verified by DNA sequencing. The EGFP-tagged beta WTs and mutants were co-transfected with the most common splice variant SCN5A [lacking a glutamine at position 1077 (Genbank accession No. AY148488)] in a 1:1 ratio and transiently expressed in HEK 293 cells for functional study as described previously.[26]

Isolation of adult rat ventricular myocytes

Animal handling practices used in this study were approved by animal use committee at the University of Wisconsin. Single ventricular myocytes were digested enzymatically from adult female Sprague-Dawley rats with collagenase and hyaluronidase, as previously described.[27] Briefly, the heart was quickly excised and mounted on a Langendorff apparatus. The heart was perfused retrogradely for 10 min at 37°C with oxygenated 1mM Ca^{+2} Ringers solution containing (in mM) 125 NaCl, 5 KCl, 2 NaH_2PO_4, 5 sodium pyruvate, 1.2 $MgSO_4$, 11 glucose, 1 $CaCl_2$ and 25 HEPES, followed by a 5mM Taurine of Ca^{+2} free Ringers solution for 5 min, and a 10 min perfusion with continuous recirculation of the same solution containing 0.5 mg/ml collagenase (type II, Worthington), and 0.35 mg/ml hyaluronidase (TypeI-S, Sigma). Then, a gradual Ca^{+2} add-back was performed to bring Ca^{+2} concentrations of the enzyme solution up to 0.5 mM. Lastly, the myocytes were maintained in 1 mM Ca^{+2} Ringers solution.

Culture and adenovirus infection of adult rat ventricular myocytes

Isolated myocytes were resuspended in Dulbecco's modified Eagle's medium (DMEM) supplemented with 5% fetal bovine serum, 50 U/ml penicillin and 50 μg/ml streptomycin and (in mM) 1 $CaCl_2$, 5 taurine,5 L-carnitine, and 5 creatine. The cells were plated on laminin-coated coverslips by incubating at 37°C, 5% CO_2-95% room air for 2 hours.[27] After 2 hours of incubation, culture medium was replaced with serum-free DMEM along with the adenovirus (Invitrogen, Carlsbad, CA) per manufacturer's instructions. Viruses were diluted in serum-free DMEM to yield a 100 MOI and cells were incubated for 24 hours. After 24 hours of incubation, the serum-free DMEM was changed and replenished every day. Two to three days later, IRES2-GFP-expressing cells, i.e. those infected by adenoviral recombinants of either β4-WT or β4-S206L, were selected for functional study.

Standard electrophysiological measurements for functional characterization

Macroscopic I_{Na} was measured using a standard whole-cell patch clamp method at a temperature of 22°–24°C as previously reported.[26] The extracellular (bath) solution contained, in mmol/L, NaCl 140, KCl 4, $CaCl_2$ 1.8, $MgCl_2$ 0.75 and HEPES 5 (pH 7.4 set with NaOH). The pipette solution contained, in mmol/L, CsF 120, CsCl 20, EGTA 2 and HEPES 5 (pH 7.4

set with CsOH). Pipettes had resistances between 1.0 and 2.0 MΩ when filled with recording solution. The standard voltage-clamp protocols are presented with the data and as described in detail previously.[28] For cardiomyocyte studies, I_{Na} were recorded in a standard whole-cell voltage-clamp model and APs were recorded in current-clamp mode using patch-clamp configuration with an Axopatch 200B patch-clamp amplifier (Axon Instruments, Foster City, CA) and pClamp 9.2 software (Axon Instruments Inc. Union City, CA). The extracellular (bath) solution contained (in mmol/L) 140 NaCl, 5.4 KCl, 1.8 CaCl2, 2.0 MgCl2, 5.0 Glucose and 5 HEPES, pH 7.4. The pipette solution contained (in mmol/L) 10 NaCl, 10 KCl, 2.0 MgCl2, 125 K-aspartate, 5.0 Glucose and 5 HEPES, pH 7.3. Cardiac myocytes were stimulated with current pulses of 1 ms duration. The currents were low-pass filtered at 5 kHz, digitized at a sampling rate of 5 kHz. I_{Na} and APs was recorded at room temperature (22°C~24°C) with pipettes resistance of 1.5~3 MΩ.

Statistical Analysis

All data points are shown as the mean value and the bars represent the standard error of the mean (S.E.M.). Determinations of statistical significance were performed using a Student *t* test for comparisons of two groups. A p-value < 0.05 was considered statistically significant. Curve fits were done using pClamp 9.2 (Axon Instruments). Additional non-linear curve fitting was performed with Origin 6.0 (Microcal Software).

RESULTS

Summary of non-synonymous mutations in the $Na_V1.5$ beta subunits

Overall, mutational analysis of the four beta subunits revealed putative pathogenic mutations in 3 of 292 cases (~1%) of SIDS. Figure 1 details the molecular characterization of the 3 identified missense mutations. An abnormal DHPLC elution profile (Figure 1A) and subsequent DNA sequencing (Figure 1B) led to the identification of a nucleotide substitution (106 G→A) producing a methionine (M) for valine (V) substitution (V36M) in *SCN3B* in a 6-week–old white female infant. A nucleotide substitution (161 A→C) causing a V54G-SCN3B missense mutation was also identified in a 6-month–old white male infant. V54G-SCN3B has been implicated recently with IVF in a 20-year-old.[24] Similarly, a nucleotide substitution (617 G→A) in *SCN4B* yielded an S206L missense mutation in a 5-month–old black male infant.

All three missense mutations involved residues conserved across a variety of species (Figure 1C) and were absent in ethnic-matched control populations, 800 reference alleles for the *SCN3B* mutations and 200 reference alleles for the *SCN4B* mutation. Figure 1D depicts the linear topology of the Na_V β3 and β4 subunits and location of the mutations. Both Na_V β3 missense mutations localized to the extracellular loop (amino acids 1–135) while the Na_V β4 mutation localized to the C-terminal, cytoplasmic region of the protein. In addition, a nucleotide substitution (28 G→A) producing a G10S amino acid substitution in the Na_V β1 subunit was identified in both an African American infant and an African American control (data not shown). Since β1-G10S was identified in both a case and a control, it was excluded from further functional studies. Due to the blinded, anonymous nature of the SIDS population-based cohort, it was not possible to obtain further information on families of the SIDS victims to establish sporadic versus familial status.

Heterologous expression of the SIDS-associated missense mutation β3-V36M

Transfected HEK-293 cells transiently expressing SCN5A + vector only, SCN5A + β3-WT, or SCN5A + β3-V36M were voltage clamped after 24h incubation. Compared to WT, β3-V36M demonstrated a marked decrease in peak I_{Na} density and accentuated persistent/late I_{Na} for β3-V36M compared to WT channels (Table 1, Figure 2A, C and Figure 3). β3-V54G

precipitated a marked attenuation in peak I_{Na} by disrupting proper trafficking of the *SCN5A*-encoded alpha subunit (data not shown).[24]

Heterologous expression of the SIDS-associated missense mutation β4-S206L

Transfected HEK-293 cells transiently expressing SCN5A + vector only, SCN5A + β4-WT, or SCN5A + β4-S206L were voltage clamped after 24h incubation. Compared with WT, β4-S206L did not affect peak I_{Na} (Table 2). However, a 7 mV positive shift of inactivation midpoint was found for β4-S206L compared to β4-WT channels (Table 2, Figure 4C). In addition, the "window" current where the activation curve overlaps the inactivation curve was also increased for β4-S206L compared to WT channels (Figure 4D). Lastly, late I_{Na} was increased significantly for β4-S206L compared to WT channels (Figure 5).

β4-S206L adenoviral transduction of adult rat ventricular myocytes

To further validate the mutant phenotype for beta subunit mutations, β4-S206L was also studied in a more native environment. IRES2-GFP-expressing isolated adult rat ventricular myocytes were voltage clamped 2–3 days following infection by adenoviral recombinants of β4-WT or β4-S206L containing the IRES2-GFP. Compared to β4-WT, ventricular myocytes infected by β4-S206L showed an increase in late I_{Na} akin to the heterologous expression studies in non cardiac cells (Figure 6A, B, E). Further, there was a marked increase in APD for β4-S206L compared to β4-WT under the current-clamp mode (Figure 6C, D, F).

DISCUSSION

This is the first study exploring the spectrum and prevalence of beta subunit mutations in SIDS. In total, 3 distinct missense mutations (2 in *SCN3B* and 1 in *SCN4B*) were identified in 292 SIDS victims (1%). These mutations were all found in residues that were well conserved across a variety of species and absent in ethnic-matched control populations. β3-V54G has been reported recently as a $Na_V1.5$ trafficking defective, loss-of-function mutation first implicated in the out-of-hospital cardiac arrest of a 20-year-old white male who was resuscitated from ventricular fibrillation during a basketball game.[24] β3-V36M displayed both $Na_V1.5$ gain- and loss-of-function properties. β4-S206L conferred a gain-of-function to $Na_V1.5$ akin to the previously published LQTS-associated SCN4B missense mutation.[25]

$Na_V1.5$ is responsible for initiating the cardiac action potential and consists of a pore-forming α subunit and, among other regulatory proteins, one or more auxiliary β subunits.[29] Mutations within *SCN5A*-encoded $Na_V1.5$ can result in various arrhythmia syndromes such as LQT3, BrS1, and autosomal recessive sick sinus syndrome. Mutations in sodium channel beta subunits have also been implicated in various diseases. For example, a mutation in *SCN1B* has been associated with febrile seizures.[30] In addition, mutations in *SCN1B* and its splice variant were identified in a cohort of 282 BrS patients and 44 CCD patients which caused $Na_V1.5$ loss-of-function *in vitro*.[22] Mutations in *SCN1B* and *SCN2B* have been associated with AF[23] while a *SCN3B* mutation has been linked to the BrS ECG phenotype.[21] Moreover, a mutation in *SCN4B* was reported in a 21-month old with LQTS and an *in vitro* LQT3-like increase in late I_{Na}.[25]

Sodium channel beta subunits play critical roles in cell adhesion, signal transduction, sodium channel plasma membrane expression and modulation of channel gating and voltage dependence.[29] Structurally, β1 and β3 subunits share sequence homology and non-covalently associate with the subunit, whereas the homologous β2 and β4 form disulfide bonds with the subunits.[29] In the present study, the β3-V36M mutation resulted in both gain- and loss-of-function channel phenotypes when compared with β3-WT, in contrast to the recently characterized β3-V54G, which is purely loss-of-function.[24] Similar to β3-V54G, β3-V36M

localizes to the extracellular loop, which is important for proper β3 membrane trafficking.[31] Deletion of the extracellular domain positively shifts steady-state inactivation and negatively shifts steady-state activation without affecting I_{Na} density.[31] Moreover, given that the artificially engineered mutation, C96A, causes the complete loss of β3 membrane expression[32] and that V54G yields a trafficking defective $Na_V1.5$ as well, it is possible that V36M may affect alpha subunit trafficking, which would explain its loss-of-function effects.

β4-S206L demonstrated increased late I_{Na} in both a heterologous system and the more native environment of adult rat cardiomyocytes. It is interesting to note that serine 206 is in close proximity to the open-channel blocker sequence from position 184–197 in the full gene product. This short sequence (KKLITFILKKTREK) is replete with hydrophobic and lysine residues which serve to block the open-channel state and induce resurgent "late sodium current" in Purkinje neurons.[32,33] This was also shown to be applicable to $Na_V1.5$.[32] It is thus conceivable that a mutation which adds another highly hydrophobic residue, leucine, close to this hydrophobic sequence may enhance its channel-blocking ability and produce a resurgent I_{Na} large enough to result in a lethal arrhythmia.

The functional studies in heterologous systems have some limitations for interpretation and application. Although localization studies have demonstrated selective targeting of the beta subunits in the cardiomyocyte,[34] it is still unclear which combinations of subunits are most critical in impacting net sodium current. While individual mutations in each of the beta subunits have been implicated in various arrhythmogenic processes, it remains challenging when performing functional studies involving beta subunits to determine which of the mutant phenotypes displayed *in vitro* may be modulated *in vivo* in the presence of the other "normal" subunits. Given these limitations, it is therefore important that we were able to reproduce the late I_{Na} findings for the β4-S206L mutation in a more native environment of cardiocytes, as well as demonstrate a marked prolongation in the cardiocyte's APD, which is the cellular substrate that predisposes to *torsades de pointes*, the hallmark dysrhythmia for the potentially lethal syndrome of LQTS. That these functionally abnormal mutations were absent in controls, in residues conserved across multiple species, and discovered in a sudden death cohort, we speculate that these infants succumbed to an infantile expression of $Na_V1.5$ dysfunction: BrS/IVF in the case of β3-V54G, LQTS for β4-S206L, and possibly a mixed/overlapping phenotype for β3-V36M.

Lastly, it is interesting to note that all three beta subunit mutations were discovered in infants outside the classic risk period for SIDS, one before two months of age, and two after four months of age. Although the age range of our assembled SIDS cohort is appropriate (1–5 months of age), this observation is consistent with our findings overall that infants found to have perturbations in the $Na_V1.5$ sodium channel complex tend to fall outside the classic two-to-four month age range.[35] Again, this raises the issue of whether the infant deaths occurring outside the critical risk period for SIDS actually stem from fundamentally different substrates, and further studies comparing different subsets of SIDS victims may elucidate this further.

CONCLUSION

In conclusion, this is the first study to implicate the sodium channel beta subunits in the pathogenesis of channelopathic SIDS. All three mutations identified were absent in controls, conserved across various species, and *in vitro* imparted abnormal gain- or loss-of-function to $Na_V1.5$. This study offers additional evidence for the crucial role of sodium channel beta subunits in the regulation of $Na_V1.5$ and expands the genetic heterogeneity for this emerging subset of channelopathic SIDS. Whether or not this particular subset (~10%) of SIDS is identifiable and preventable requires much further investigation.

Acknowledgments

This work was supported by the University of Wisconsin Cellular and Molecular Arrhythmia Research Program (J.C.M.), the Mayo Clinic Windland Smith Rice Comprehensive Sudden Cardiac Death Program (M.J.A.), the Established Investigator Award from the American Heart Association (to M.J.A.), and the grants HD42569 (to M.J.A.) and HL71092 (to J.C.M.) from National Institutes of Health, USA.

Abbreviations

BrS	Brugada Syndrome
IVF	idiopathic ventricular fibrillation
LQTS	Long QT syndrome
SCN5A	voltage-gated sodium channel
SIDS	sudden infant death syndrome

References

1. Krous HF, Beckwith JB, Byard RW, et al. Sudden infant death syndrome and unclassified sudden infant deaths: a definitional and diagnostic approach. Pediatrics 2004;114:234–238. [PubMed: 15231934]
2. Mathews TJ, MacDorman MF. Infant mortality statistics from the 2004 period linked birth/infant death data set. Natl Vital Stat Rep 2007;55:1–32. [PubMed: 17569269]
3. Tester DJ, Ackerman MJ. Sudden infant death syndrome: how significant are the cardiac channelopathies? Cardiovasc Res 2005;67:388–396. [PubMed: 15913580]
4. Tester DJ, Dura M, Carturan E, et al. A mechanism for sudden infant death syndrome (SIDS): stress-induced leak via ryanodine receptors. Heart Rhythm 2007;4:733–739. [PubMed: 17556193]
5. Schwartz PJ, Stramba-Badiale M, Segantini A, et al. Prolongation of the QT interval and the sudden infant death syndrome. N Engl J Med 1998;338:1709–1714. [PubMed: 9624190]
6. Schwartz PJ, Priori SG, Dumaine R, et al. A molecular link between the sudden infant death syndrome and the long- QT syndrome. N Engl J Med 2000;343:262–267. [PubMed: 10911008]
7. Brugada R, Hong K, Dumaine R, et al. Sudden death associated with short-QT syndrome linked mutations in HERG. Circulation 2004;109:30–35. [PubMed: 14676148]
8. Arnestad M, Crotti L, Rognum TO, et al. Prevalence of long-QT syndrome gene variants in sudden infant death syndrome. Circulation 2007;115:361–367. [PubMed: 17210839]
9. Ackerman MJ, Siu BL, Sturner WQ, et al. Postmortem molecular analysis of SCN5A defects in sudden infant death syndrome. JAMA 2001;286:2264–2269. [PubMed: 11710892]
10. Ackerman MJ. The long QT syndrome: ion channel diseases of the heart. Mayo Clin Proc 1998;73:250–269. [PubMed: 9511785]
11. Bennett PB, Yazawa K, Makita N, George AL Jr. Molecular mechanism for an inherited cardiac arrhythmia. Nature 1995;376:683–685. [PubMed: 7651517]
12. Wang Q, Shen J, Splawski I, et al. SCN5A mutations associated with an inherited cardiac arrhythmia, long QT syndrome. Cell 1995;80:805–811. [PubMed: 7889574]
13. Antzelevitch C, Brugada P, Brugada J, et al. Brugada Syndrome: a decade of progress. Circ Res 2002;91:1114–1118. [PubMed: 12480811]
14. Vatta M, Ackerman MJ, Ye B, et al. Mutant caveolin-3 induces persistent late sodium current and is associated with long-QT syndrome. Circulation 2006;114:2104–2112. [PubMed: 17060380]
15. Cronk LB, Ye B, Kaku T, et al. Novel mechanism for sudden infant death syndrome: persistent late sodium current secondary to mutations in caveolin-3. Heart Rhythm 2007;4:161–166. [PubMed: 17275750]
16. Van Norstrand DW, Valdivia CR, Tester DJ, et al. Molecular and functional characterization of novel glycerol-3-phosphate dehydrogenase 1 like gene (GPD1-L) mutations in sudden infant death syndrome. Circulation 2007;116:2253–2259. [PubMed: 17967976]

17. London B, Michalec M, Mehdi H, et al. Mutation in glycerol-3-phosphate dehydrogenase 1 like gene (GPD1-L) decreases cardiac Na+ current and causes inherited arrhythmias. Circulation 2007;116:2260–2268. [PubMed: 17967977]
18. Cheng J, Van Norstrand DW, Medeiros-Domingo A, et al. α1-syntrophin mutations identified in sudden infant death syndrome cause an increase in late cardiac sodium current. Circ Arrhythmia Electrophysiol 2009;2:667–676.
19. Ueda K, Valdivia CR, Medeiros-Domingo A, et al. Syntrophin mutation associated with long QT syndrome through activation of the nNOS-SCN5A macromolecular complex. Proc Natl Acad Sci U S A 2008;105:9355–9360. [PubMed: 18591664]
20. Mohler PJ, Rivolta I, Napolitano C, LeMaillet G, Lambert S, Priori SG. E1053K mutation causing Brugada syndrome blocks binding to ankyrin-G and expression of Nav1.5 on the surface of cardiomyocytes. Proc Natl Acad Sci U S A 2004;101:17533–17438. [PubMed: 15579534]
21. Hu D, Barajas-Martinez H, Burashnikov E, et al. A mutation in the beta3 subunit of the cardiac sodium channel associated with Brugada ECG phenotype. Circ Cardiovasc Genet 2009;2:270–278. [PubMed: 20031595]
22. Watanabe H, Koopmann TT, Le SS, et al. Sodium channel β1 subunit mutations associated with Brugada syndrome and cardiac conduction disease in humans. J Clin Invest 2008;118:2260–2268. [PubMed: 18464934]
23. Watanabe H, Darbar D, Kaiser DW, et al. Mutations in sodium channel beta1 and beta2 subunits associated with atrial fibrillation. Circ Arrhythmia Electrophysiol 2009;2:268–275.
24. Valdivia CR, Medeiros-Domingo A, Ye B, et al. Loss of function mutation of the SCN3B-encoded sodium channel {beta}3 subunit associated with a case of idiopathic ventricular fibrillation. Cardiovasc Res 2009:cvp417.
25. Medeiros-Domingo A, Kaku T, Tester DJ, et al. SCN4B-encoded sodium channel beta4 subunit in congenital long-QT syndrome. Circulation 2007;116:134–142. [PubMed: 17592081]
26. Nagatomo T, Fan Z, Ye B, et al. Temperature dependence of early and late currents in human cardiac wild- type and long Q-T DeltaKPQ Na+ channels. Am J Physiol 1998;275:H2016–2024. [PubMed: 9843800]
27. Chung KY, Kang M, Walker JW. Contractile regulation by overexpressed ETA requires intact T tubules in adult rat ventricular myocytes. Am J Physiol Heart C 2008;294:H2391–2399.
28. Tan B-H, Valdivia CR, Rok BA, et al. Common human *SCN5A* polymorphisms have altered electrophysiology when expressed in Q1077 splice variants. Heart Rhythm 2005;2:741–747. [PubMed: 15992732]
29. Meadows LS, Isom LL. Sodium channels as macromolecular complexes: implications for inherited arrhythmia syndromes. Cardiovasc Res 2005;67:448–458. [PubMed: 15919069]
30. Wallace RH, Scheffer IE, Parasivam G, et al. Generalized epilepsy with febrile seizures plus: mutation of the sodium channel subunit SCN1B. Neurology 2002;58:1426–1429. [PubMed: 12011299]
31. Yu EJ, Ko S, Lenkowski PW, Pance A, Patel MK, Jackson AP. Distinct domains of the sodium channel beta3-subunit modulate channel-gating kinetics and subcellular location. Biochem J 2005;392:519–526. [PubMed: 16080781]
32. Wang GK, Edrich T, Wang SY. Time-dependent block and resurgent tail currents induced by mouse beta4154–167 peptide in cardiac Na+ channels. J Gen Physiol 2006;127:277–289. [PubMed: 16505148]
33. Grieco TM, Malhotra JD, Chen C, Isom LL, Raman IM. Open-channel block by the cytoplasmic tail of sodium channel beta4 as a mechanism for resurgent sodium current. Neuron 2005;45:233–244. [PubMed: 15664175]
34. Maier SK, Westenbroek RE, McCormick KA, Curtis R, Scheuer T, Catterall WA. Distinct subcellular localization of different sodium channel alpha and beta subunits in single ventricular myocytes from mouse heart. Circulation 2004;109:1421–1427. [PubMed: 15007009]
35. Van Norstrand DW, Cheng J, Valdivia CR, et al. Spectrum and prevalence of mutations in the sodium channel macromolecular complex in SIDS. Heart Rhythm 2009;6:S86. [abstract]. [PubMed: 19541550]

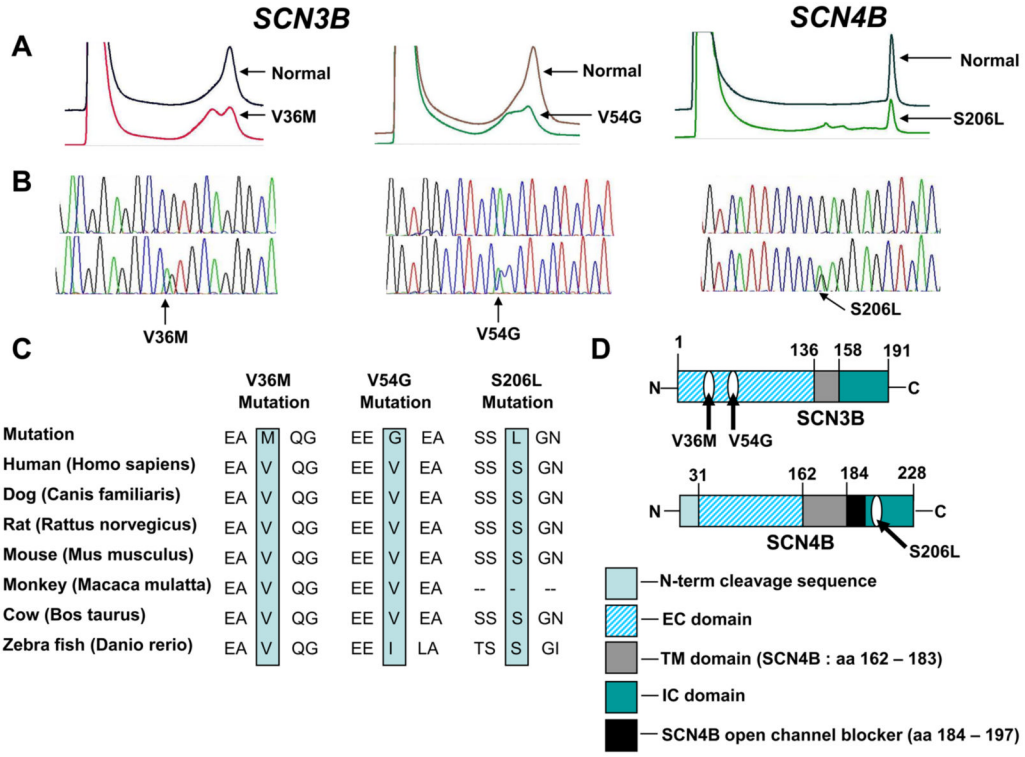

Figure 1. Identification of beta subunit mutation in SIDS

Depicted are the A) DHPLC profiles (normal, above and abnormal, below) and B) DNA sequencing chromatograms for each mutation. C) Sequence homologies are compared for the three mutations. D) Illustrated is the linear topology of the β3 and β4 subunits with mutation localization. EC = extracellular. TM = transmembrane. IC = intracellular.

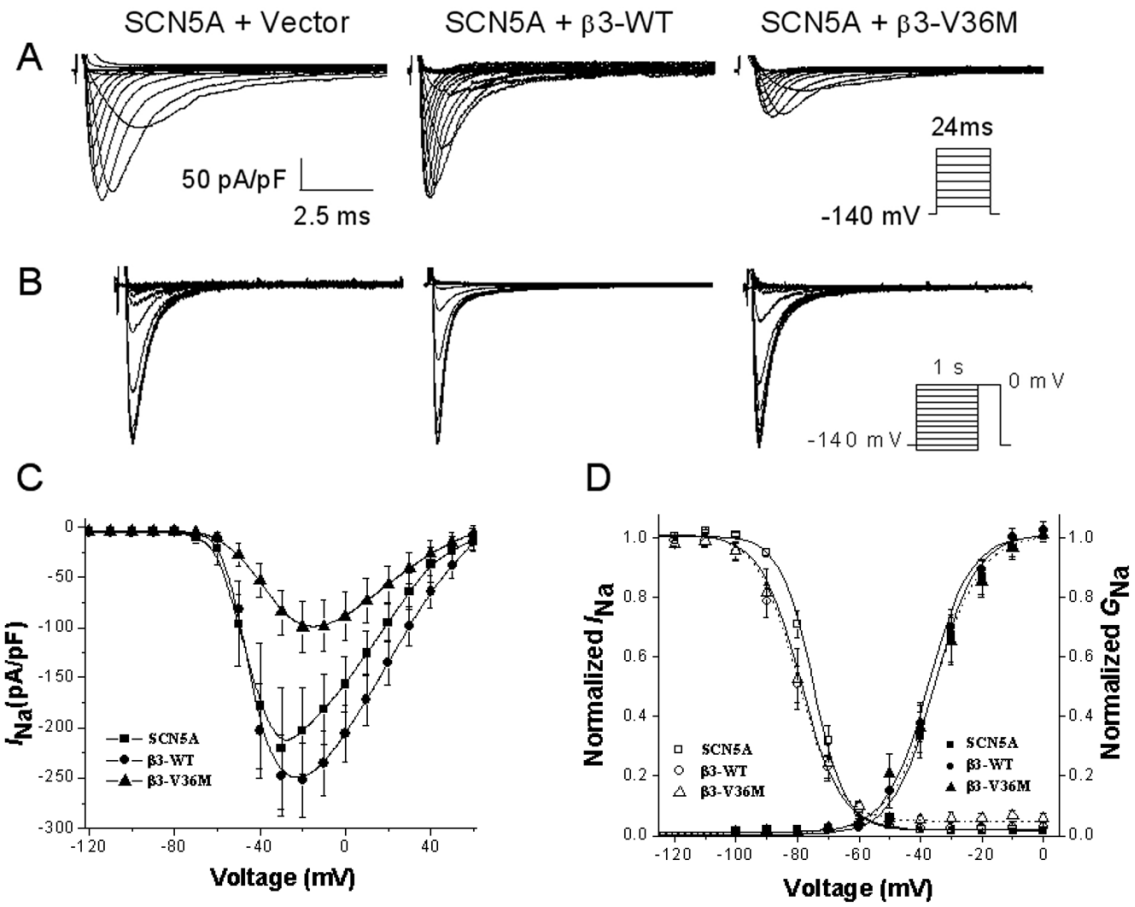

Figure 2.

Functional characterizations of IRES2-GFP-β3-WT and IRES2-GFP-β3-V36M co-transfected with the *SCN5A*-encoded Nav1.5 α-subunit in HEK-293 cells. (A, B) Whole-cell current traces from representative experiments of SCN5A + Vector (left panel), SCN5A + β3-WT (middle panel) and SCN5A + β3-V36M (right panel) in response to the voltage clamp protocol that is diagrammed in the inset. (C) Current-voltage relationships for SCN5A + Vector, SCN5A + β3-WT and SCN5A + β3-V36M. Peak I_{Na} was normalized to membrane capacitance (pA/pF). (D) Steady-state voltage dependence of activation (right plot) and inactivation (left plot) for SCN5A + Vector, SCN5A + β3-WT and SCN5A + β3-V36M. Data are means of measurements, and the lines are Boltzmann fits with n cell numbers and parameters of the fit shown in Table 1.

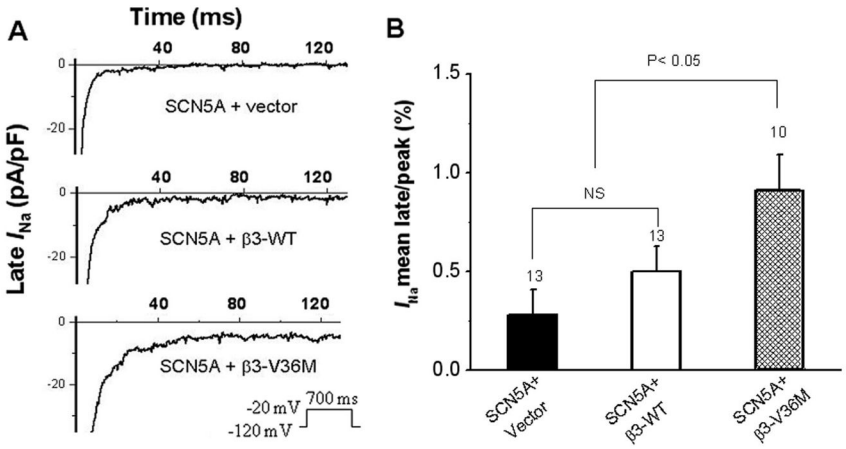

Figure 3.

Comparison of the late I_{Na} of SCN5A with either β3-WT or β3-V36M in HEK-293 cells. (A) Examples of late I_{Na} for SCN5A + Vector, SCN5A + β3-WT and SCN5A + β3-V36M elicited by a test depolarization pulse from −120 mV to −20 mV for 700 ms. Late was I_{Na} normalized to cell capacitance, and presented in pA/pF. (B) Summary of late I_{Na} normalized to peak $I_{Na.}$ After leak-subtraction, the late I_{Na} was measured as the mean between 600 ms and 700 ms after the initiation of the depolarization. The number of cells is indicated above the bar.

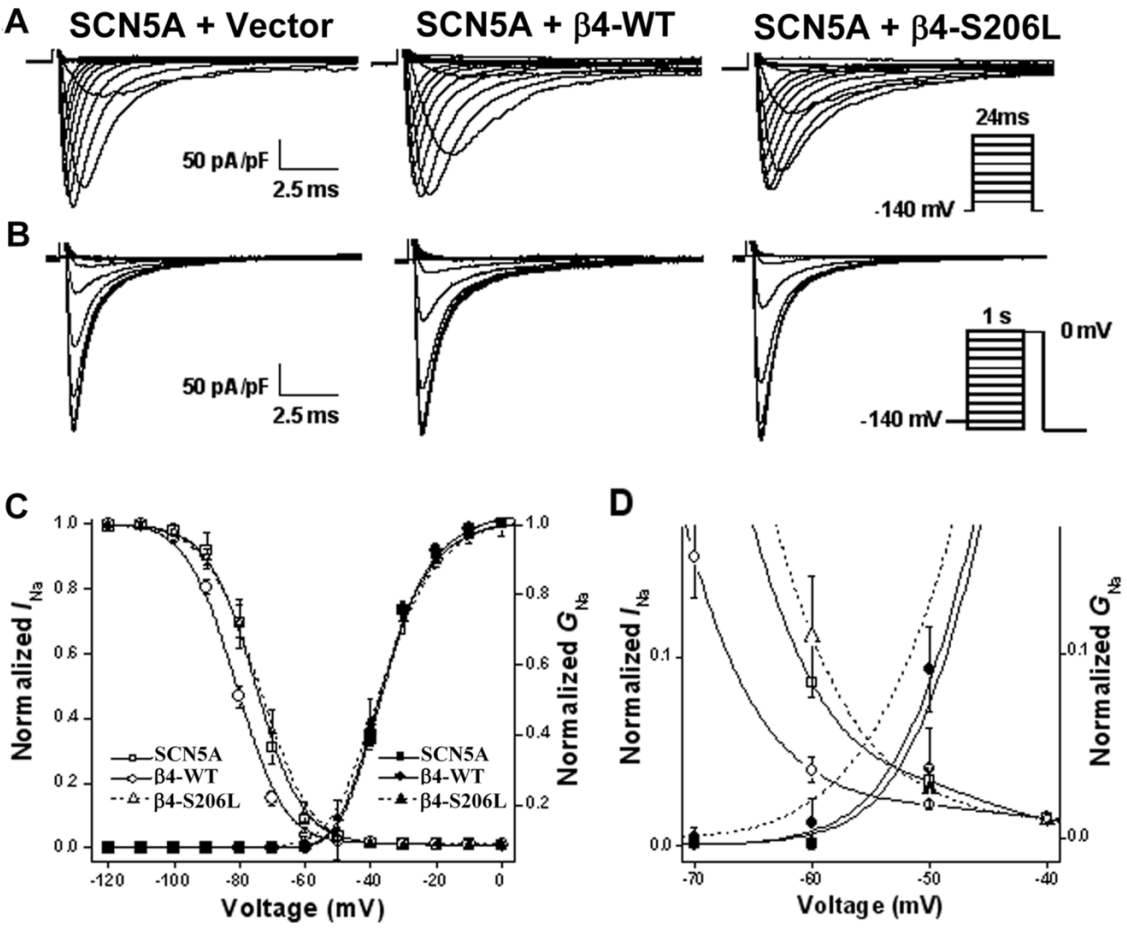

Figure 4.

Functional characterizations of IRES2-GFP-β4-WT and IRES2-GFP-β4-S206L co-transfected with the *SCN5A*-encoded Nav1.5 α-subunit in HEK-293 cells. (A, B) Whole-cell current traces from representative experiments of SCN5A + Vector (left panel), SCN5A + β4-WT (middle panel) and SCN5A + β4-S206L (right panel) in response to the voltage clamp protocol that is diagrammed in the inset. (C) Steady-state voltage dependence of activation (right plot) and inactivation (left plot) of SCN5A + Vector, SCN5A + β4-WT and SCN5A + β4-S206L. Data are means of measurements, and the lines are Boltzmann fits with n numbers and parameters of the fit shown in Table 2. (D) Enlarged scale from C to better show the "window" current where the activation curves overlap the inactivation curves.

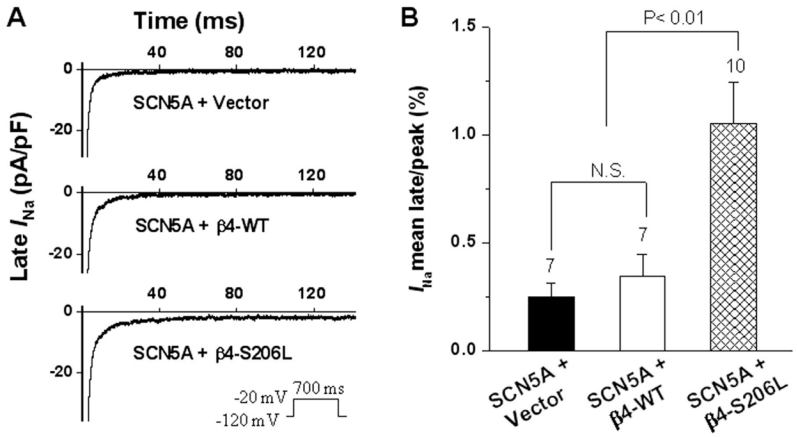

Figure 5.

Comparison of the late I_{Na} of SCN5A with either β4-WT or β4-S206L in HEK-293 cells. (A) Examples of late I_{Na} for SCN5A + Vector, SCN5A + β4-WT and SCN5A + β4-S206L elicited by a test depolarization pulse from −120 mV to −20 mV for 700 ms (here only 140 ms is shown). Late I_{Na} was normalized to cell capacitance, and presented in pA/pF. (B) Summary of late I_{Na} normalized to peak $I_{Na.}$ After leak-subtraction, the late I_{Na} was measured as the mean between 600 ms and 700 ms after the initiation of the depolarization. The number of cells is indicated above the bar.

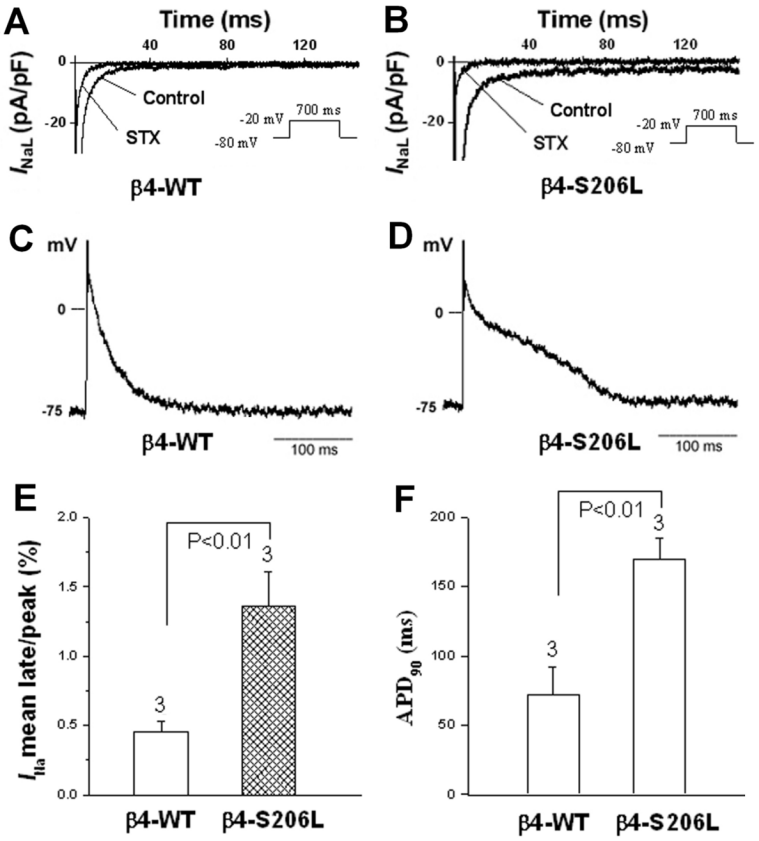

Figure 6.

Whole cell patch-clamp recording from isolated adult rat ventricular myocytes infected by adenoviral recombinants of IRES2-GFP-β4-WT and IRES2-GFP-β4-S206L. (A, B) Representative late I_{Na} for β4-WT and β4-S206L elicited by a test depolarization pulse from −80 mV to −20 mV for 700 ms (here only 150 ms is shown) in absence and presence of saxitoxin (STX) (1μM) in the voltage clamp mode. (C, D) Representative action potential recording from myocytes infected by adenoviral recombinants of IRES2-GFP-β4-WT and IRES2-GFP-β4-S206L in a current-clamp mode. (E) Summary of late I_{Na} normalized to peak I_{Na} for IRES2-GFP-β4-WT and IRES2-GFP-β4-S206L, in which the late I_{Na} was measured as the mean inward current between 600 and 700 ms after the initiation of the depolarization by subtracting a trace in the presence of 1uM STX from a trace obtained earlier in the absence of STX.(F) Average APD90 (AP duration at 90% repolarization) for β4-WT and β4-S206L. The number of cells is indicated above the bar.

Table 1

Voltage-dependent gating parameters of β3-WT and β3-V36M

	Peak I_{Na}		Activation			Inactivation		Recovery			
Samples	**pA/pF**	***n***	**$V_{1/2}$(mV)**	**K**	***n***	**$V_{1/2}$ (mV)**	***n***	**τ_f (ms)**	**τ_s (ms)**	**As (%)**	***n***
SCN5A + Vector	−230 ± 49	13	−36 ± 2	4.7	7	−75 ± 1	8	1.5 ± 0.3	54 ± 9	25 ± 2	8
SCN5A + β3-WT	−245 ± 43	26	−39 ± 1	4.7	20	−79 ± 1#	21	1.4 ± 0.2	44 ± 7	24 ± 2	14
SCN5A + β3-V36M	−102±24*#	13	−36 ± 2	5.0	11	−80 ± 1#	11	1.5 ± 0.2	43 ± 9	28 ± 1	9

The fitted values of voltage-dependent gating parameters represent the mean ± SEM for number of cells *n* in the table. These parameters were obtained from fitting the individual experiments as in Figure 2C&D to the appropriate model equations.

For the Boltzmann fits the parameters of $V_{1/2}$ are the midpoint of activation and inactivation.

#P< 0.05 vs SCN5A + Vector.

*P< 0.05 vs β3-WT.

Table 2

Voltage-dependent gating parameters of β4-WT and β4-S206L

	Peak I_{Na}		Activation			Inactivation			Recovery		
Samples	**pA/pF**	***N***	**$V_{1/2}$(mV)**	**K**	***n***	**$V_{1/2}$ (mV)**	***n***	**τ_f (ms)**	**& tau;s (ms)**	**As (%)**	***n***
SCN5A + Vector	−240 ± 38	10	−38 ± 1.0	4.3 ± 0.1	9	−75 ± 2.2	9	1.7 ± 0.2	35 ± 3.2	24 ± 0.9	8
SCN5A + β4-WT	−274 ± 56	12	−40 ± 0.8	4.4 ± 0.2	9	−81 ± 0.9	8	1.5 ± 0.3	29 ± 5.8	22 ± 2.3	8
SCN5A +β4-S206L	−253 ± 18	12	−41 ± 1.7	4.6 ± 0.3	11	−74 ± 1.9	11	1.5 ± 0.2	34 ± 4.2	21 ± 2.3	8

The fitted values of voltage-dependent gating parameters represent the mean ± SEM for number of cells *n* in the table. These parameters were obtained from fitting the individual experiments as in Figure 4C to the appropriate model equations.

For the Boltzmann fits the parameters of $V_{1/2}$ are the midpoint of activation and inactivation.

*P<0.05 vs. SCN5A + β4-S206L and SCN5A + Vector.